Chapter 5 - Injection Molding Metallic Glass

After determining that the $Zr_{35}Ti_{30}Be_{27.5}Cu_{7.5}$ alloy shows the most promise of any known alloy for TPF processes requiring large strains, we set out to demonstrate injection molding of a metallic glass for the first time. This chapter draws heavily on "Injection Molding Metallic Glass" published in Scripta Materialia [A. Wiest, J.S. Harmon, M.D. Demetriou, R.D. Conner, W.L. Johnson, Scripta Mater. 60 (2009) 160]. Advances in alloy development produced the $Zr_{35}Ti_{30}Be_{27.5}Cu_{7.5}$ alloy with (crystallization - glass transition temperature) = ΔT = 165 °C. This alloy's large supercooled liquid region (SCLR) provides the longest processing times and lowest processing viscosities of any metallic glass and was injection molded using tooling based on plastic injection molding technology. Injection molded beams and die cast beams were tested in three-point bending. The average modulus of rupture (MOR) was found to be similar while injection molded beams had a smaller standard deviation in MOR.

Bulk metallic glasses (BMG) are high strength, high hardness, highly elastic, low modulus, low melting temperature materials with no crystalline order that have been the subject of extensive research in recent years [1-4]. Because of their low melting temperature they are easily processed using conventional vacuum die casting and suction casting techniques. These methods require processing that is sufficiently fast to avoid crystallization, and alloys with high glass forming ability (GFA) are generally preferred. Die cast parts have somewhat unreliable mechanical properties because of porosity that often exists in the specimens due to the high flow velocities required to fill the mold cavity [5]. The cooling requirements of die casting bound the dimensions of die cast parts to no larger than can be cooled sufficiently fast to avoid crystallization and no

smaller than can be quickly filled. Parts with complex geometries, thin sections, and high aspect ratios are difficult to obtain with die casting.

Thermoplastic forming decouples the forming and cooling processes because it is carried out in the SCLR between the glass transition temperature, T_g, and the crystallization temperature, T_x. In the SCLR a BMG forming alloy exists as a viscous, deeply undercooled liquid. The viscosity of the alloy follows a hyper-Arrhenius function of temperature [6] and crystallization is forestalled due to the sluggish kinetics in the deeply undercooled liquid. Much longer processing times are available in the SCLR than are available when casting from the molten state because the alloy is resistant to crystallization below T_x. Die casting processes must shape and cool the alloy in seconds to tens of seconds while processing in the SCLR allows hundreds to thousands of seconds for forming and cooling. Time temperature transformation (TTT) diagrams measure the time to crystallization of an alloy held isothermally at a given temperature. Viscosity plots measure the Newtonian viscosity of an alloy held isothermally at a given temperature. Figure 5.1 combines data from these two kinds of plots to show attainable viscosity for a given processing time for three alloys commonly used in thermoplastic forming experiments and the alloy used in this experiment, $Zr_{35}Ti_{30}Be_{27.5}Cu_{7.5}$ [6-9]. This plot is a viscosity time transformation plot, ηTT. Good TTT data upon heating is not available in the literature for $Pd_{43}Ni_{20}Cu_{27}P_{20}$ so cooling TTT data was used for the Pd alloy in the Figure 5.1. Crystallization times are known to be shorter for heating TTT plots compared to cooling TTT plots for the same alloy. Accordingly, the true heating ηTT plot for the Pd alloy should be moved to shorter times. It is clearly seen that the $Zr_{35}Ti_{30}Be_{27.5}Cu_{7.5}$ alloy has the lowest processing viscosity for a wide range of

processing times. Interpolation of viscosities not directly measured was done using the fit suggested by Johnson et al. [6].

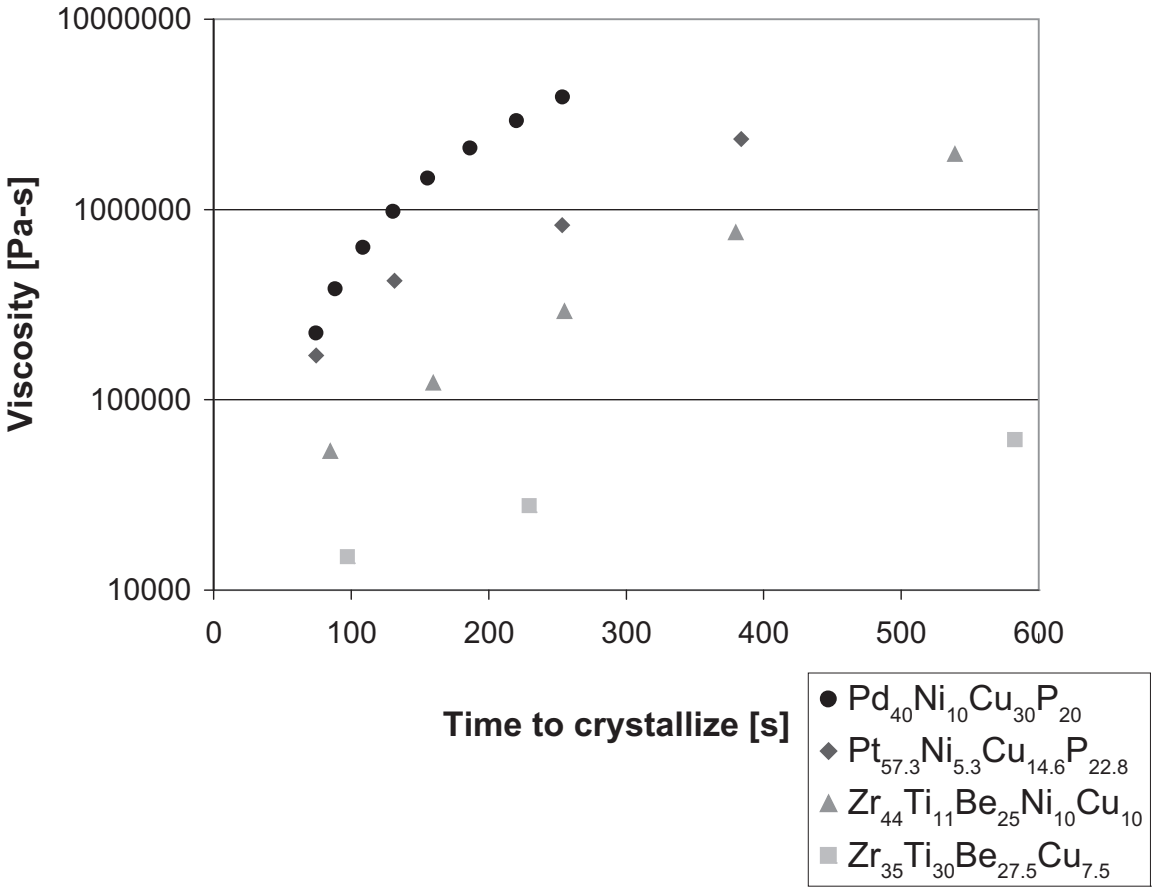

Figure 5.1: Time to crystallization versus viscosity plot for four thermoplastically processable alloys. This plot combines TTT and viscosity versus time data found in references [6-9] to show available processing time for a given viscosity for the alloys.

The decreasing viscosity and longer processing times available in the SCLR allow metallic glasses to be processed in ways similar to plastics which are not possible with crystalline metal alloys. Nanometer scale features with high aspect ratios have been formed in the SCLR by pressing metallic glasses into etched wells of semiconductor materials [10]. Glassy powders have been consolidated in the SCLR to form net shaped parts [11]. Hot extrusion has been demonstrated using Zr based alloys [12] and blow molding experiments using relatively low pressures yielded hemispheres with high

quality surface finish [13]. An additional benefit to processing BMG in the SCLR is the decoupling of forming and cooling steps which allows formation of parts larger than the critical casting thickness of the alloy.

A conventional processing method used in the plastics industry that has not previously been successfully demonstrated with BMG is injection molding. This is in part due to the limited viscosities and processing times available in the SCLR of known alloys. Recent discovery of alloys with SCLR ($\Delta T = T_x - T_g$) as high as 165 ^oC makes BMG injection molding a possibility [14].

A basic injection molding machine has a heated reservoir in which plastic feedstock is softened, a piston or plunger to apply pressure to the feedstock, a nozzle or gate to restrict the flow of plastic when necessary and a mold into which the plastic is forced to form a part. A schematic drawing of the setup used in this experiment is shown in Figure 5.2b. Typical operating temperatures and pressures are 175 °C – 350 °C and 35 MPa - 150 MPa, respectively. Softened plastics used for injection molding usually have a viscosity of ~ 10^3 Pa-s.

$Zr_{44}Ti_{11}Be_{25}Cu_{10}Ni_{10}$, $Pd_{43}Ni_{10}Cu_{27}P_{20}$ and $Pt_{57.5}Ni_{5.3}Cu_{14.7}P_{22.5}$ were among the most thermoplastically processable alloys known, reaching viscosities of ~ 10^5 Pa-s in the SCLR before onset of crystallization. The alloy used in this experiment, $Zr_{35}Ti_{30}Be_{27.5}Cu_{7.5}$, can reach viscosities in the SCLR of ~ $3*10^4$ Pa-s at 420 °C with ~ 230 s available for thermoplastic processing at that temperature [15]. This is an order of magnitude lower viscosity than is attainable in the SCLR of previously reported metallic glasses [16-18]. However, when compared to the viscosity of plastics used for injection molding, it is an order of magnitude higher viscosity. A modified injection molding

setup was created to accommodate the higher temperatures and pressures necessary to force the more viscous $Zr_{35}Ti_{30}Be_{27.5}Cu_{7.5}$ supercooled liquid into a mold cavity.

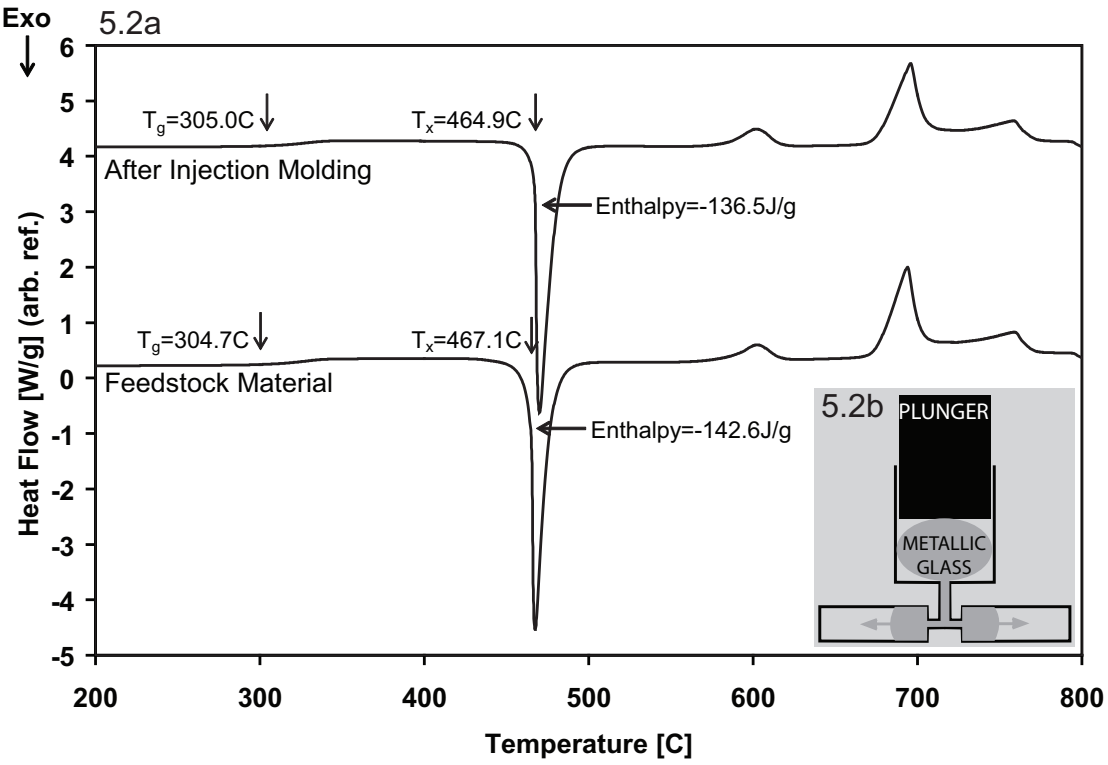

Figure 5.2: 2a - 20 ^{o}C/min DSC scans of feedstock material and injection molded specimen. The injection molding process appears to have had little effect on the thermodynamic properties measured in the DSC. Inset 2b - Schematic drawing of the modified injection molding setup consisting of a plunger, gates, and a heated mold and reservoir. The dimensions of the mold cavities are 2mm x 10mm x 20mm and 1.5mm x 10mm x 20mm.

The $Zr_{35}Ti_{30}Be_{27.5}Cu_{7.5}$ feedstock material was made using >99.9% pure elements and melted thoroughly in an arc melter under a Ti-gettered argon atmosphere. Each ingot was flipped and remelted multiple times to ensure chemical homogeneity. Ingots with more than 0.1% deviation from initial weighed mass after melting were discarded. Die casting was done by radio frequency heating the alloy in a quartz nozzle and injecting the molten alloy into a copper mold using argon pressure. The amorphous nature of all material was determined using X-ray diffraction and DSC. Mechanical testing was

performed on an Instron 4204 Load Frame at a constant displacement rate of 0.5mm/min in a three-point bending geometry to determine MOR.

Suitable feedstock material was also required for the injection molding process. Various methods were tested to create amorphous feedstock material and the effect on ΔT was measured in the DSC at 20 K/min. We noticed large variations in ΔT depending on the method used. The results are summarized in Table 5.1. To test the variation of ΔT with rod diameter, samples were RF melted and cast into copper molds or water quenched in quartz tubes had ΔT values ranging from 136 °C to 170 °C but there was no systematic variation with rod diameter and the ΔT = 170 °C was only obtained once. We also tried melting the alloy in a furnace so the melting temperature could be controlled more carefully and identical diameter rods were formed. The ΔT values ranged from 153 °C to 165 °C but the results were not systematic. Arc melted buttons showed the most uniformity in ΔT and were chosen as the feedstock material. We removed the thin crystalline layer on the side of the ingot in contact with the copper hearth with a diamond saw and collected X-ray diffraction data on the cut samples to ensure they were completely amorphous.

A schematic drawing of the modified injection molding setup can be found in Figure 5.2b. The experimental setup consisted of a plunger used to apply force, a 19mm diameter x 20mm tall heated reservoir in which BMG feedstock material was brought to the processing temperature, an 8mm diameter x 3mm tall vertical channel opening into two perpendicular channels with dimensions 5mm x 2mm x 2mm long which restricted the flow of material into the mold cavity. The heated mold cavity on the left in Figure

5.2b is 10mm x 2mm x 60mm long and the one on the right is 10mm x 1.5mm x 60mm long.

Table 5.1: Effects of rod diameter and overheating above melt temperature on ΔT as well as variation in arc melted button ΔT are tabulated. Temperatures given in °C.

	T_g	T_x	ΔT
Furnace melted samples			
7mm quartz 1235 °C	304	459	155
7mm quartz 1200 °C	303	459	156
7mm quartz 1145 °C	304	457	153
7mm quartz 930 °C	302	467	165
RF melted samples			
3mm Cu mold	305	441	136
6mm quartz	305	452	147
10mm quartz	307	477	170
15mm quartz	306	450	144
Arc Melted Ingots			
Ingot 7	305	469	164
Ingot 9	298	464	166
Ingot 11	299	467	168
Ingot 12	302	465	163
Ingot 13	306	466	160
Ingot 15	304	464	160
Ingot 16	304	467	163
Ingot 18	303	467	164
Ingot 21	306	469	163
Ingot 23	307	466	159
Ingot 25	304	468	164
Ingot 26	305	467	162
Average Arc Melted Ingots	**304**	**467**	**163**
Standard Deviation	**2.7**	**1.7**	**2.6**

A photograph of injection molding attempts is shown in Figure 5.3. The most successful run was accomplished when the mold and glassy feedstock material were heated to 420 °C with a force of 300 MPa applied to the material in the reservoir for two minutes. The material completely filled the larger mold cavity and a 0.2mm diameter flashing was formed along the perimeter due to insufficient clamping pressure. The

material that filled this cavity underwent more than 1000% strain. Minimal polishing with 320 grit sand paper removed the surface oxide layer and the beam formed in the large mold cavity was found to be glassy using X-ray diffraction. The flow was terminated in the smaller cavity due to crystallization of material near the heating element. Figure 5.3c shows the most successful metallic glass part; Figures 5.3a and 5.3b illustrate two less successful attempts, and Figure 5.3d is a part made of polyethylene shown for reference. The short fill shown in Figure 5.3a was due to the plunger binding in the reservoir. Note the parabolic flow front visible on both sides of the part.

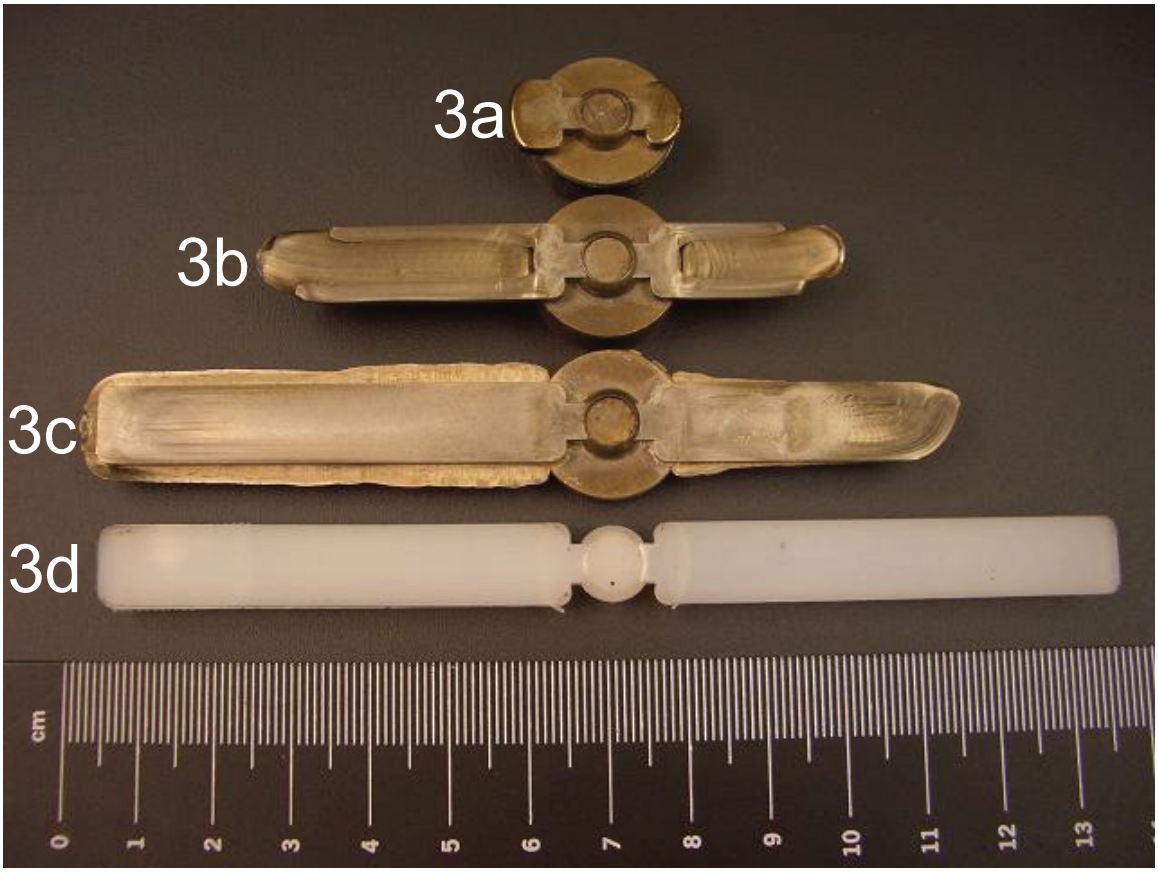

Figure 5.3: Photograph of injection molded parts. The top part (5.3a) was processed at 410 ^{o}C with an applied pressure of 140 MPa but the plunger jammed. The second part (5.3b) was processed at 385 ^{o}C with an applied pressure of 300 MPa for three minutes. The third part (5.3c) was processed at 420 ^{o}C with an applied pressure of 300 MPa for two minutes. The fourth part (5.3d) made of polyethylene was processed at 210 ^{o}C with an applied pressure of 35 MPa for one minute.

Using the velocity distribution of a viscous fluid flowing in a cylindrical channel assuming stick boundary conditions and laminar flow we obtain $v = -\frac{1}{4\eta}\frac{\Delta P}{\Delta x}(R^2 - r^2)$, where v is the velocity of a lamina, η is the viscosity, ΔP is the pressure differential of the pipe, Δx is a displacement in the direction of flow, R is the diameter of the pipe, and r is the radial distance from the center of the pipe. A similar equation results for an ellipse where the lamina are elliptical cylinders instead of circular. In the limiting case of a rectangular channel, a parabolic velocity distribution is found away from the corners. The observed flow front suggests laminar flow into the mold cavity. Laminar flow is important, as it reduces the formation of voids and other flaws which weaken the part. The part shown in Figure 5.3b was processed at too low a temperature, resulting in a processing viscosity that was too high as indicated by "river marks" or flow lines. Despite the large thermal stability of $Zr_{35}Ti_{30}Be_{27.5}Cu_{7.5}$, approximately 10 times more force is required to form the metallic glass part than was used to form a polyethylene part of the same geometry. The polyethylene part filled both mold cavities at a processing temperature of 250 °C and a pressure of 35 MPa, while those of the BMG are 420 °C and 300 MPa.

We were able to process metallic glass parts with 10 times higher processing viscosity than polyethylene by using a higher force. It is natural to wonder if perhaps even more force could be applied to alloys with higher processing viscosities and achieve similar flow. Up to a certain point this strategy works but shortens mold life. If too high a strain rate is imposed at a given viscosity, non-Newtonian flow results and shear banding can occur in the SCLR.

The availability of injection molding as a potential forming process for metallic glass parts allows for the formation of parts greater than the critical casting thickness of the parent alloy. Injection molding is carried out at temperatures much lower than die casting which may improve the mold lifetime. Since processing is accomplished in the laminar flow regime, higher quality and more reliable parts can be fabricated than with current die casting technology.

DSC scans of the feedstock material and a section of the injection molded beam are overlaid in Figure 5.2a. The ΔT value of the injection molded material is slightly smaller than the feedstock material and the enthalpies of crystallization are nearly identical.

The injection molded plate was sectioned into 2mm x 2mm x 20mm beams for mechanical testing in three-point bending. The modulus of rupture (MOR, σ_{max}) was determined for 12 beams and compared to die cast specimens of the same dimension using the formula $\sigma_{max} = \frac{3FL}{2ab^2}$ s where F = applied force, $a = b$ = 2mm, L = distance between bottom supports of the three-point bending setup = 13mm. The MOR equation for a square beam is derived in Derivation 9.

The die cast specimens were cut from three 2mm x 10mm x 20mm plates. Figure 5.4 shows the results of the three-point bend tests. Twelve specimens of each fabrication method were tested, with MOR = 2.923 ± 0.065 GPa for injection molding and MOR = 2.879 ± 0.240 GPa for die casting. Note that the average MOR is nearly identical for both processing methods while the standard deviation of the injection molded specimens is 73% less than that of the die cast specimens. This suggests that injection molding produces parts with more reliable mechanical properties than their die cast counterparts.

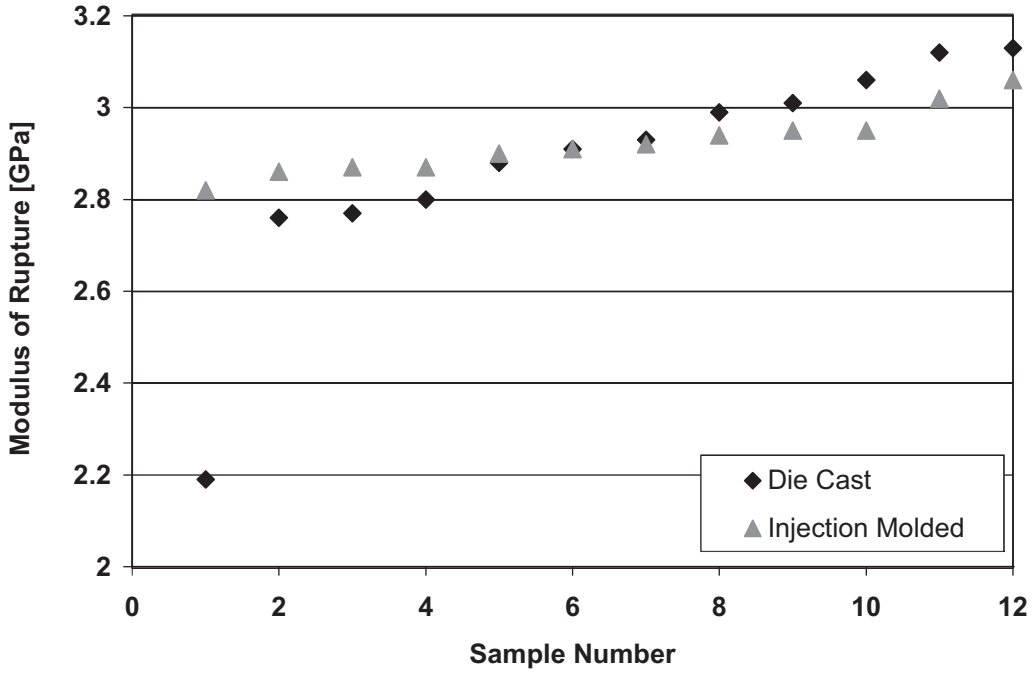

Figure 5.4: Plot of modulus of rupture values for injection molded and die cast samples. Die cast modulus of rupture = (2.879 ± 0.240)GPa. Injection molding modulus of rupture = (2.923 ± 0.065)GPa.

The discovery of the $Zr_{35}Ti_{30}Be_{27.5}Cu_{7.5}$ alloy with viscosity in the SCLR as low as 10^4 Pa-s allowed injection molding of a metallic glass to be demonstrated. Tooling based on plastic injection molding machines was used, but modified to allow for the higher temperatures and pressures necessary to process the more viscous metallic glass. The material underwent strains greater than 1000% at a temperature of 420 °C and a pressure of 300 MPa applied for two minutes and formed a part 2mm x 10mm x 60mm. The injection molded part was tested mechanically in three-point bending and showed MOR equivalent to that of a die cast specimen with a standard deviation of MOR 73% less than that of die cast specimens of the same composition and dimension. The ability to injection mold high strength metal parts using methods similar to existing plastics

technology could greatly reduce processing costs, and will be the subject of future investigation.

Special thanks to Doug Hofmann, Rebecca Stevens, Glenn Garrett, Jin-Yoo Suh, and Joe Schramm for valuable discussion and heroic help quenching the 420 °C massive mold.

Chapter 5 References

[1] A.L. Greer, E. Ma, MRS Bull. 32 (2007) 611.
[2] W.L. Johnson, MRS Bull. 24 (1999) 42.
[3] A. Inoue, Acta Mater. 48 (2000) 279.
[4] W.L. Johnson, JOM 54 (2002) 40.
[5] K.J. Laws, B. Gun, M. Ferry, Mat. Sci. Eng. A 425 (2006) 114.
[6] W.L. Johnson, M.D. Demetriou, J.S. Harmon, M.L. Lind, K. Samwer, MRS Bull. 32 (2007) 644.
[7] B.A. Legg, J. Schroers, R. Busch, Acta Mater. 55 (2007) 1109.
[8] J.F. Löffler, J. Schroers, W.L. Johnson, Appl. Phys. Lett. 77 (2000) 681.
[9] T. Waniuk, J. Schroers, W.L. Johnson, Phys. Rev. B 67 (2003) 184203.
[10] J. Schroers, Q. Pham, A. Desai, J. Microelectromech. S. 16 (2007) 240.
[11] J. Degmova, S. Roth, J. Eckert, H. Grahl, L. Schultz, Mat. Sci. Eng. A 375 (2004) 265.
[12] K.S. Lee, Y.W. Chang, Mat. Sci. Eng. A-Struct. 399 (2005) 238.
[13] J. Schroers, Q. Pham, A. Peker, N. Paton, R.V. Curtis, Scripta Mater. 57 (2007) 341.
[14] A. Wiest, G. Duan, M.D. Demetriou, L.A. Wiest, A. Peck, G. Kaltenboeck, B. Wiest, W.L. Johnson, Acta Mater. 56 (2008) 2625.
[15] G. Duan, A. Wiest, M.L. Lind, J. Li, W.K. Rhim, W.L. Johnson, Adv. Mater. 19 (2007) 4272.
[16] G.J. Fan, H.J. Fecht, E.J. Lavernia, Appl. Phys. Lett. 84 (2004) 487.
[17] R. Busch, E. Bakke, W.L. Johnson, Acta Mater. 46 (1998) 4725.
[18] H. Kato, T. Wada, M. Hasegawa, J. Saida, A. Inoue, H.S. Chen, Scripta Mater. 54 (2006) 2023.